Kalman Smoothing for better RFID Landslide Monitoring

Arthur Charléty[1], Olivier J.J. Michel[2], and Mathieu Le Breton[3]

[1] Université Grenoble Alpes, Université Savoie Mont Blanc, CNRS, IRD, Université Gustave Eiffel, ISTerre, Grenoble, France
[2] Univ. Grenoble-Alpes, CNRS, Grenoble-INP, GIPSA Lab, 38000 Grenoble
[3] Géolithe, Crolles, France

***Abstract*—The use of Radio-Frequency Identification (RFID) in Earth Sciences has been growing in the recent years, notably for landslide monitoring using phase-of-arrival localization schemes. In this article, an Extended Kalman Filtering approach is presented to exploit RFID phase data for landslide displacement monitoring. The filtering is based on a stochastic Langevin equation for the state-space model, introducing a heuristic coupling based on the mechanical continuity of the landslide material. This helps correct measurement biases and deal with missing data in the tracking of multiple tags. The Kalman state covariance matrix is a useful indicator of the tags localization quality. It can be exploited to discriminate true displacements from multipath-induced artifacts. Phase unwrapping is performed implicitly through the state model.**

***Index Terms*—RFID, Kalman, Landslides, Sensor Fusion**

I. Introduction

The use of RFID in Earth Sciences has been growing in the recent years [1], with notable applications in landslide monitoring [2]. RFID tags are low-cost and versatile devices that can be easily deployed, and represent cheap and dense solutions for displacement monitoring. This was already demonstrated in both 1D and 2D long-term monitoring [3], [4], with centimeter accuracy and weather robustness.

The counterpart of these advantages is the need to handle phase noise and ambiguity [5]. The high amount of data and its redundancy, both in space and time, implies a high number of different sensors with inhomogeneous data sampling, variable noise levels and the risk of measurement bias (caused by multipath interference for example [6]). For such datasets, fusion approaches based on Kalman Filters or Extended Kalman Filters (EKF) have been widely investigated for the localization of moving tags [7]. EKF enable to work with missing data and variable measurement errors, which makes them particularly fit for redundant and noisy datasets. Moreover, the continuity of displacements can be implemented in the EKF physical model to further increase the robustness of the filter, like with RTK-GNSS localization [8]. Kalman-based sensor coupling is vastly demonstrated for GNSS sensor fusion [9], [10]. Data fusion from multiple sensors is the main motivation for applying EKF to RFID tag localization [11] [12]. In [13], [14] an EKF is used to fuse data from multiple antennas in order to perform indoor localization. In a real-world scenario, [15] demonstrates RSSI and phase data fusion to improve absolute ranging and relative displacement estimation.

EKF are also widely used in Earth Sciences, notably in landslide monitoring scenarios.They often address data scarcity through sensor fusion [16], [17], or to synthesise different observables and models [18], [19].

In general, combining RFID tags considerably enhances the precision of phase results, notably using an average operator [20]. In this work, we aim to improve RFID data combination with a Kalman-based approach. We address data scarcity and varying accuracy by exploiting data redundancy and physical heuristics in order to link multiple tags together. Namely, we implement the continuity of position and velocity both in space and time at the observation scale (about 1-10 m). The main specificity of the proposed method lies in the coupling of multiple tags at different positions, based on the concept of landslide kinematic element [21]. The approach we propose yields an improved and model-based phase unwrapping, as well as data completion and fusion. Furthermore it provides an estimate of the quality of the localization estimation, which is of great importance from a user point-of-view. This work is the first attempt at applying the EKF to improve long-term, outdoor and slow-moving RFID monitoring.

II. Experimental Setup

The Harmalière landslide (Sinard, France) is a slow moving landslide located near Grenoble in the western Pre-Alps. It is investigated by many research projects [22]. The RFID setup, installed in 2020, consists of 4 reader antennas and 32 tags spread in a 30m by 30m investigated zone. Tacheometry reference measurements are frequently performed. The experimental setup (see Fig. 1) was described and validated elsewhere [2]–[4], as well as signal processing methods for data availability improvement [5], and showed centimeter-accuracy in 2D over year-long monitoring.

III. Model and Kalman filter

Measurement setup A set of M antennas (4 in our setup) at respective positions $\mathbf{x}_a^m$, $m \in \{1, \dots, M\}$ are spread at the border of the landslide area (see Fig.1A). The antenna of index m estimates a phase propagation delay for each single tag at position $\mathbf{x}$. This phase is:

$$\Phi_m = \frac{4\pi f}{c} d_m + \Phi_{off} \ ,$$

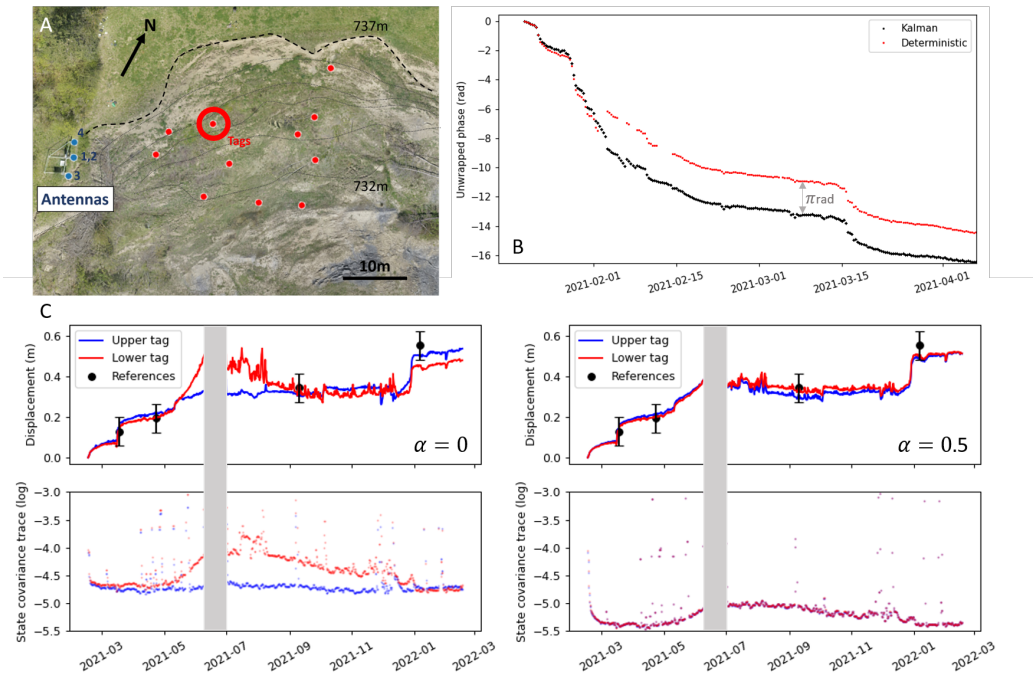

FIG. 1 A : Aerial view of the landslide equipped with RFID monitoring. B : Example of phase series, unwrapped by the Kalman filter or by a deterministic approach [5]. C : (Top) Displacement for two tags on the same support at different heights (highlighted tag in A). The two tags were chosen among 32 to be those with the best quality of recorded data. Left: $\alpha = 0$ (no coupling between tag velocities). Right: $\alpha = 0.5$ (equal contribution of mutual velocities). The black dots represent reference measurement, with the corresponding error bar. (Bottom) Trace of the Kalman covariance state matrix for each tag.

where Φ_{off} holds for the phase offset and $d_m = \|\mathbf{x} - \mathbf{x}_a^m\|$. All phases are only observable modulo π (8 cm ambiguity) due to RFID reader constraints. A first order approximation with respect to the tag displacement gives:

$$\delta d_m = \mathbf{u}_m^T \delta\mathbf{x} + o(\|\delta\mathbf{x}\|), \quad \delta\Phi_m \approx \tfrac{4\pi f}{c}\mathbf{u}_m^T\delta\mathbf{x} \qquad (1)$$

where $\mathbf{u}_m = \frac{\mathbf{x}-\mathbf{x}_a^m}{\|\mathbf{x}-\mathbf{x}_a^m\|}$ is a unit norm vector. For this single tag and M antennas, we get:

$$\delta\mathbf{\Phi} = [\delta\Phi_1, \ldots, \delta\Phi_M]^T = \frac{4\pi f}{c}\begin{pmatrix}\mathbf{u}_1^T\\ \vdots \\ \mathbf{u}_M^T\end{pmatrix}\delta\mathbf{x} = \mathbf{K}\delta\mathbf{x}\,, \qquad (2)$$

Where $\mathbf{K} \in \mathbb{R}^{d\times M}$ and d is the space dimension (3 in our case). The classical MSE estimation of the tag position change, given a set of M phase measurements leads to solve the normal equation:

$$\mathbf{K}\mathbf{K}^T\delta\mathbf{x} = \mathbf{K}\delta\mathbf{\Phi}\,.$$

Assuming that phase measurements errors are Gaussian distributed, this solution matches with the maximum likelihood estimate. It provides an unbiased estimate of $\delta\mathbf{x}$ and with a variance equal to $(\mathbf{K}\mathbf{K}^T)^{-1}$.

This approach exhibits two problems: first it requires that the antenna/tag geometry ensures that $\mathbf{K}\mathbf{K}^T$ has full rank (as studied in [3]), and the variance depends on the conditioning of this latter matrix. This builds the motivation for developing an alternative approach relying on Kalman filtering. To that end, a state equation is required, usually directly related to the displacement physical model.

In early-warning and monitoring applications, empirical or kinematic landslide models are often used [23], [24]. A simple and approximate model is derived below.

Physical model Let Z_t be a state vector in $\mathbb{R}^{2dN}$, constructed from both positions $\mathbf{P}_t$ and velocities $\mathbf{V}_t$ of a set of N tags at time t:

$$Z_t = \begin{pmatrix}\mathbf{P}_t\\ \mathbf{V}_t\end{pmatrix} = (\mathbf{x}_t^{1\,T} \ldots \mathbf{x}_t^{N\,T}\mathbf{v}_t^{1\,T} \ldots \mathbf{v}_t^{N\,T})^T\,.$$

We propose a model constructed from both the fundamental principle of dynamics in physics and from an heuristics stating that close enough tags will have coupled trajectories. Consequently, we assume that all movements are due to random forces or accelerations. Note that although gravity is the major long-term driving force constraining downwards displacements, local landslide block activity generates displacements in all directions (for example, block rotation generates upward movement). Thus velocities behave like Wiener-Levy processes, and the system will follow the following Langevin equation [25]:

$$d\begin{pmatrix}\mathbf{P}_t\\ \mathbf{V}_t\end{pmatrix} = \begin{pmatrix}\mathbf{0} & C\\ \mathbf{0} & \mathbf{0}\end{pmatrix}\begin{pmatrix}\mathbf{P}_t\\ \mathbf{V}_t\end{pmatrix}dt + \begin{pmatrix}0_{Nd}\\ \sqrt{\beta}\mathbf{1}_{Nd}\end{pmatrix}\begin{pmatrix}0_{Nd}\\ d\mathbf{w}_t\end{pmatrix}\,, \qquad (3)$$

where $\mathbf{0}$ and C are $Nd \times Nd$ matrices, 0_{Nd} and $\mathbf{1}_{Nd}$ are constant (resp. 0 ad 1) vectors of dimension Nd. $\mathbf{w}_t$ is the

Nd dimensional Wiener Levy process with unit covariance matrix (assuming that all driving forces are independent and have identical diffusion constants). C is the velocity coupling matrix whose expression will be discussed later. $\sqrt{\beta}$ entails inertial mass and power of the driving force. It represents the diffusion coefficient of the process. From Eq. (3) the Fokker-Planck ordinary differential equation followed by the covariance matrix of Z_t is derived and after integrating on the interval $[0, t]$, we get [25], [26]:

$$\Gamma_z(t) = \beta \begin{pmatrix} \frac{t^3}{3} CC^T & \frac{t^2}{2} C \\ \frac{t^2}{2} C^T & t\mathbb{I}_{Nd \times Nb} \end{pmatrix} . \quad (4)$$

The above expression of $\Gamma_z(t)$ is of major interest as it accounts for both the decrease of the model reliability when the time t between two consecutive observations increases, and for the statistical dependence of position an velocity estimates. This latter dependence is related to the fact that velocities are not observed but derived from the position estimates.

Velocity coupling matrix: Arguing that tags near each other should have similar velocities (because they belong to the same kinematic elements [21]), the following structure for C is proposed:

$$[C]_{ii} = (1-\alpha) \quad [C]_{ij} = \frac{\alpha}{\sigma_j^2} \mathrm{e}^{-\frac{d_{ij}}{\lambda}} \quad i,j \in \{1, \ldots, N\} \quad , \quad (5)$$

where λ accounts for the characteristic distance above which tags are considered to have possibly independent velocities, and σ_j^2 will be the tag j estimated velocity error variance. This allows to lower the influence of tags whose velocity is badly estimated. Note that C is time dependent (d_{ij} and σ_j vary with time). Forcing C to be the identity will lead to a solution where each tag position and velocity may be tracked independently from each other.

State equation: All previous results and equations lead to the state equation (integral form of Eq. (3), between t and $t' > t$):

$$Z_{t'} = \begin{pmatrix} \mathbf{I} & C_t \\ \mathbf{0} & \mathbf{I} \end{pmatrix} Z_t + \gamma_{t'} = AZ_t + \gamma_{t'} , \quad (6)$$

where $\gamma_{t'}$ is a $2Nd$-dimensional white noise with correlation matrix $\Gamma_z(t - t')$ defined by Eq. (4). Note that the larger the time elapsed between two observations (at t and t'), the larger the covariance matrix of the state noise $\gamma_{t'}$.

Observation equation: It is derived from Eq. (2), to which some observation noise is added. The measurement covariance matrix of the observation noise $\xi_{t'}$, noted Γ_Φ, depends upon the instrument used to estimate $\delta\mathbf{\Phi}$ (see [4], [5] for more details). Finally, by assuming that $\delta\mathbf{x}_{t'} \approx (t' - t)\mathbf{V}_t$ (this is satisfied if the velocities vary slowly on the interval $[t, t']$), we get:

$$\delta\mathbf{\Phi}_{t'} = \begin{pmatrix} \mathbf{0} & (t'-t)\mathbf{K}_t \end{pmatrix} Z_{t'} + \xi_{t'} = H_t Z_{t'} + \xi_{t'} . \quad (7)$$

Although this equation is linear at each step, it is important to notice that H_t varies with t.

Remarks: In practice, forcing row and column of index k of Γ_Φ to take very large values at some time instants where measurements from antenna k are missing allows the Kalman filter to rely only on the state equation at these time instants; actually, it can be shown that the Kalman gain k-th component will be thus forced to a near zero value. Nonetheless, the velocity coupling term C_t will still force some local ensemble movement. The problem of phase unwrapping disappears in the Kalman formulation as the 'modulo π' term is determined by considering the forecast:

$$\delta\hat{\mathbf{\Phi}}(t'|t) = H\hat{Z}_{t'|t} .$$

This quantity is estimated at t' from the system observed until time t only. Setting both state and noise covariance matrices is critical, as it deals with the precision/robustness tradeoff. Choosing β is therefore critical. On the contrary, setting $C = \mathbf{I}$ in Γ_z has a lower importance in practice, and will be adopted in order to simplify the Kalman filter implementation.

The terms σ_j and d_{ij} are replaced in Eq. (5) by the estimated velocity error covariance for tag j and by $|\hat{\mathbf{x}}_i - \hat{\mathbf{x}}_j|$ respectively, estimated at time t. The derivation of the Kalman filter equation is then classical and is not detailed is this short article.

We have derived an Extended Kalman Filtering approach including sensor state coupling, and accounting for position-velocity error correlation. Next section will comment on simple real-data results.

IV. Results and discussion

Figure 1C presents displacement results from a pair of tags, with their *a posteriori* (after Kalman filtering) error covariance estimation ; results for two different values of α (different C matrices) are compared. The grey bar represents a data gap caused by hardware failure. Two main phases of activity stand out : March 2021 and January 2022, with peak velocities of 2 cm / day.

As expected, the covariance estimation shows a strong sensibility to missing data, with extremely high values that are not shown here. Except from these (useful) values which can be filtered out, the variation of the covariance trace informs the user about the overall quality of the localization.

In the case where $\alpha = 0$ ($C = \mathbf{I}$) it can be considered as a proxy for detecting interference phenomena or defective material. The presented pair of tags should share approximately the same displacement, as they are positioned on the same object. Nonetheless we see a drift of the lower tag occurring from May to October 2021, with a temporary displacement difference of 20cm between the two tags. This drift, along with the strong increase in state covariance, is most likely a sign of radiofrequency interference [27]. This interpretation is confirmed by the received signal strength indicator which strongly decreases during the same period. As shown in [3] for the same setup, this phenomenon mostly impacts tags positioned closer to the ground. The state covariance estimate is a tool for assessing the confidence of a result. In the present case, the apparent displacement shown by the lowest tag around June 2021 can be discarded, it is identified as an artifact due to the important state covariance increase.

In the case of $\alpha = 0.5$ the drift between tags is diminished, as the model imposes a partially-shared velocity. It can be shown that the choice of $\alpha > 0$ implies a decrease in the *a posteriori* covariance, and this theoretical result is validated by observation. However this higher precision is obtained at the cost of a decreased robustness of the filter : it is less stable with respect to a departure between model and reality. We also note that the drift of the lower tag is propagated to the upper tag, generating a displacement artifact on both tags for the whole period of May to October 2021. Using a higher number of tags as well as a different value for α should be a way of solving this issue [28].

An example of model-based phase unwrapping is shown in Fig. 1B. The velocity propagation implemented in the model allowed for a correct unwrapping compared to deterministic methods [5].

The coupling between tags relies on the concept of kinematic element, stating that landslide blocks stand out with coherent displacements. In practice this assumption is often verified in the current geomorphological environment [21]. Nonetheless, the distance-based correlation does not fully correspond to the landslide block situation : close tags could behave differently if they're on a different block. Implementing a correlation function based on tag clusters could improve the results.

V. Conclusion

Extended Kalman Filters applied to long-term outdoor RFID data allow to complete data gaps with multi-tag guidance thanks to a position-velocity model, and to perform model-based phase unwrapping. The Kalman state covariance matrix is a usefull indicator of the localization quality. It can be exploited to discriminate true displacements from multipath-induced artifacts.

References

[1] M. Le Breton, F. Liébault, L. Baillet, A. Charléty, É. Larose, and S. Tedjini, "Dense and long-term monitoring of earth surface processes with passive rfid—a review," *Earth-Science Reviews*, p. 104225, 2022.

[2] M. Le Breton, L. Baillet, E. Larose, E. Rey, P. Benech, D. Jongmans, F. Guyoton, and M. Jaboyedoff, "Passive radio-frequency identification ranging, a dense and weather-robust technique for landslide displacement monitoring," *Engineering geology*, vol. 250, pp. 1–10, 2019.

[3] A. Charléty, M. Le Breton, E. Larose, and L. Baillet, "2d phase-based rfid localization for on-site landslide monitoring," *Remote Sensing*, vol. 14, no. 15, p. 3577, 2022.

[4] M. Le Breton, L. Baillet, E. Larose, E. Rey, P. Benech, D. Jongmans, and F. Guyoton, "Outdoor uhf rfid: Phase stabilization for real-world applications," *IEEE Journal of Radio Frequency Identification*, vol. 1, no. 4, pp. 279–290, 2017.

[5] A. Charléty, M. L. Breton, L. Baillet, and E. Larose, "RFID landslide monitoring : long-term outdoor signal processing and phase unwrapping," 3 2023.

[6] E. Giannelos, E. Andrianakis, K. Skyvalakis, A. G. Dimitriou, and A. Bletsas, "Robust rfid localization in multipath with phase-based particle filtering and a mobile robot," *IEEE Journal of Radio Frequency Identification*, vol. 5, no. 3, pp. 302–310, 2021.

[7] P. Henriques Abreu, J. Xavier, D. Castro Silva, L. P. Reis, and M. Petry, "Using kalman filters to reduce noise from rfid location system," *The Scientific World Journal*, vol. 2014, 2014.

[8] Y. Gao, Y. Gao, B. Liu, and Y. Jiang, "Enhanced fault detection and exclusion based on kalman filter with colored measurement noise and application to rtk," *GPS Solutions*, vol. 25, pp. 1–13, 2021.

[9] S. Sirtkaya, B. Seymen, and A. A. Alatan, "Loosely coupled kalman filtering for fusion of visual odometry and inertial navigation," in *Proceedings of the 16th International Conference on Information Fusion*, pp. 219–226, IEEE, 2013.

[10] G. Falco, M. Pini, and G. Marucco, "Loose and tight gnss/ins integrations: Comparison of performance assessed in real urban scenarios," *Sensors*, vol. 17, no. 2, p. 255, 2017.

[11] Q. Yang, D. G. Taylor, M. B. Akbar, and G. D. Durgin, "Analysis of kalman filter-based localization for himr rfid systems," *IEEE Journal of Radio Frequency Identification*, vol. 3, no. 3, pp. 164–172, 2019.

[12] V. Magnago, L. Palopoli, A. Buffi, B. Tellini, A. Motroni, P. Nepa, D. Macii, and D. Fontanelli, "Ranging-free uhf-rfid robot positioning through phase measurements of passive tags," *IEEE Transactions on Instrumentation and Measurement*, vol. 69, no. 5, pp. 2408–2418, 2019.

[13] S. Sarkka, V. V. Viikari, M. Huusko, and K. Jaakkola, "Phase-based uhf rfid tracking with nonlinear kalman filtering and smoothing," *IEEE Sensors Journal*, vol. 12, no. 5, pp. 904–910, 2011.

[14] A. Bekkali, H. Sanson, and M. Matsumoto, "Rfid indoor positioning based on probabilistic rfid map and kalman filtering," in *Third IEEE International Conference on Wireless and Mobile Computing, Networking and Communications (WiMob 2007)*, pp. 21–21, IEEE, 2007.

[15] A. J. Hoffman and N.-P. Bester, "Rss and phase kalman filter fusion for improved velocity estimation in the presence of real-world factors," *IEEE Journal of Radio Frequency Identification*, vol. 5, no. 1, pp. 75–93, 2020.

[16] J. Cai, G. Liu, H. Jia, B. Zhang, R. Wu, Y. Fu, W. Xiang, W. Mao, X. Wang, and R. Zhang, "A new algorithm for landslide dynamic monitoring with high temporal resolution by kalman filter integration of multiplatform time-series insar processing," *International Journal of Applied Earth Observation and Geoinformation*, vol. 110, p. 102812, 2022.

[17] Q. Tan, P. Wang, J. Hu, P. Zhou, M. Bai, and J. Hu, "The application of multi-sensor target tracking and fusion technology to the comprehensive early warning information extraction of landslide multi-point monitoring data," *Measurement*, vol. 166, p. 108044, 2020.

[18] N. Zhang, W. Zhang, K. Liao, H.-h. Zhu, Q. Li, and J. Wang, "Deformation prediction of reservoir landslides based on a bayesian optimized random forest-combined kalman filter," *Environmental Earth Sciences*, vol. 81, no. 7, pp. 1–14, 2022.

[19] F. Lu and H. Zeng, "Application of kalman filter model in the landslide deformation forecast," *Scientific Reports*, vol. 10, no. 1, pp. 1–12, 2020.

[20] M. Le Breton, É. Larose, L. Baillet, Y. Lejeune, and A. van Herwijnen, "Monitoring snowpack swe and temperature using rfid tags as wireless sensors," *EGUsphere*, pp. 1–24, 2022.

[21] W. H. Schulz, J. A. Coe, P. P. Ricci, G. M. Smoczyk, B. L. Shurtleff, and J. Panosky, "Landslide kinematics and their potential controls from hourly to decadal timescales: Insights from integrating ground-based insar measurements with structural maps and long-term monitoring data," *Geomorphology*, vol. 285, pp. 121–136, 2017.

[22] S. Fiolleau, D. Jongmans, G. Bièvre, G. Chambon, P. Lacroix, A. Helmstetter, M. Wathelet, and M. Demierre, "Multi-method investigation of mass transfer mechanisms in a retrogressive clayey landslide (harmalière, french alps)," *Landslides*, vol. 18, pp. 1981–2000, 2021.

[23] S. Bernardie, N. Desramaut, J.-P. Malet, M. Gourlay, and G. Grandjean, "Prediction of changes in landslide rates induced by rainfall," *Landslides*, vol. 12, pp. 481–494, 2015.

[24] E. Intrieri, T. Carlà, and G. Gigli, "Forecasting the time of failure of landslides at slope-scale: A literature review," *Earth-science reviews*, vol. 193, pp. 333–349, 2019.

[25] L. Arnold, *Stochastic differential equations, Theory and Applications*. Wiley Interscience, 1973.

[26] A. Jazwinski, *Stochastic Processes and Filtering Theory*. Dover, 2008.

[27] A. M. Whitney, J. M. Parker, Z. C. Kratzer, J. T. Fessler, and J. G. Whitney, "Reducing rf distance error by characterizing multipath," *IEEE Transactions on Instrumentation and Measurement*, vol. 68, no. 9, pp. 3329–3338, 2018.

[28] K. H. Eom, S. J. Lee, Y. S. Kyung, C. W. Lee, M. C. Kim, and K. K. Jung, "Improved kalman filter method for measurement noise reduction in multi sensor rfid systems," *Sensors*, vol. 11, no. 11, pp. 10266–10282, 2011.